Sheffield Hallam University

SiGeSn growth studies using reduced pressure chemical vapor deposition towards optoelectronic applications

WIRTHS, S., BUCA, D., IKONIC, Z., HARRISON, Paul <http://orcid.org/0000-0001-6117-0896>, TIEDEMANN, A. T., HOLLÄNDER, B., STOICA, T., MUSSLER, G., BREUER, U., HARTMANN, J. M., GRÜTZMACHER, D. and MANTL, S.

Citation:

SiGeSn Growth Studies Using Reduced Pressure Chemical Vapor Deposition Towards Optoelectronic Applications

S. Wirths[1]*, D. Buca[1], Z. Ikonic[2], P. Harrison[2], A.T. Tiedemann[1], B. Holländer[1], T. Stoica, G. Mussler[1], U. Breuer[3], J.M. Hartmann[4], D. Grützmacher[1], and S. Mantl[1]

[1]Peter Grünberg Institute (PGI 9-IT) and JARA-FIT, Forschungszentrum Juelich, 52425, Germany

[2]Institute of Microwaves and Photonics, School of Electronic and Electrical Engineering, University of Leeds, Leeds LS2 9JT, United Kingdom

[3]Central Institute for Engineering, Electronics and Analytics (ZEA-3) Forschungszentrum Juelich, 52425, Germany

[4]CEA, LETI, MINATEC Campus, 17 rue des Martyrs, 38054 Grenoble, France

ABSTRACT:

In this contribution, we propose a laser concept based on a double heterostructure consisting of tensile strained Ge as the active medium and SiGeSn ternaries as cladding layers. Electronic band-structure calculations were used to determine the Si and Sn concentrations yielding a type I heterostructure with appropriate band-offsets (50 meV) between strained Ge and SiGeSn. Reduced pressure chemical vapor deposition system was employed to study the laser structure growth. Detailed analyses regarding layer composition, crystal quality, surface morphology and elastic strain are presented. A strong temperature dependence of the Si and Sn incorporation have been obtained, ranging from 4-19 at.% Si and 4-12 at.% Sn (growth temperatures between 350°C and 475°C). The high single crystalline quality and low surface roughness of 0.5-0.75 nm demonstrate that our layers are suitable for heterostructure laser fabrication.

*corresponding author : s.wirths@fz-juelich.de; Tel.: +49 2461 61-3149

Fax: +49 2461 61-2940

1. Introduction

Photonic integrated circuits on Si and nanoelectronics devices, as Tunnel Field Effect Transistors [1,2], would strongly benefit from direct bandgap group IV semiconductors. Since the energy difference in the conduction band edges at the L and Γ valleys of Ge is 0.14 eV only [3], Ge-based materials are the most promising candidates to achieve the desired indirect to direct bandgap transition. Recently, both theoretical and experimental studies have shown that Ge can be band-engineered into a quasi-direct gap semiconductor via tensile strain or the incorporation of Sn [4–6]. It has been predicted that a direct bandgap can be achieved for a tensile deformation of 2% in Ge without heavy n-type doping [7]. However, the use of strained Ge (sGe) as active laser medium demands also the development of suitable barrier layers in order to confine the charge carriers and achieve population inversion. The group IV SiGeSn alloys are ideal candidates to be employed as cladding layers due to the possibility of modifying the lattice constant and bandgap, independently [8,9]. Due to the low solid solubility of Sn in Ge ($< 1\%$) [10] and the strong tendency for surface segregation of Sn, low growth temperatures have to be used. However, significantly higher temperatures are used for Si epitaxy than for Ge and especially GeSn growth. Hence, finding the appropriate temperature window for single crystalline SiGeSn growth is very challenging. The first SiGeSn growth studies have been reported by Bauer *et al.* [11] employing SiH_3GeH_3 precursor for Si and Ge and SnD_4 as Sn precursor using an ultra-high vacuum chemical vapor deposition (UHV-CVD) reactor. Whereas the first layers grown on Si(100) were amorphous, lattice-matched $Ge_{1-x-y}Si_xSn_y$ with $x \leq 0.2$ and $y \leq 0.05$ were deposited on Ge(100), recently [12].

Based on electronic band-structure calculations, we first address the Si and Sn concentration ranges that would yield $Si_xGe_{1-x-y}Sn_y$ ternary alloys with appropriate band-offsets to tensely strained Ge. Then, we present the epitaxial growth of $Si_xGe_{1-x-y}Sn_y$ layers on

3

Si(100) and on Ge virtual substrates (VS). The aim is to demonstrate the feasibility of growing the laser heterostructures suggested by simulations.

2. Experimental details

For the growth studies we employ a 200 mm AIXTRON Tricent® Reduced Pressure CVD (RP-CVD) tool with a showerhead technology [13,14]. Si_2H_6, Ge_2H_6 (10% in H_2), $SnCl_4$ and N_2 as the carrier gas are used for the required low temperature epitaxial growth. Prior to epitaxial growth, an *ex-situ* HF-vapor etching of native oxide followed by an *in-situ* pre-epi bake at about 850°C were performed. The stoichiometry and thickness of the grown layers were extracted by means of Rutherford Backscattering Spectrometry (RBS). RBS/C measurements were performed by means of a Tandetron accelerator with 1.4 MeV He^+ ions using a backscattered angle of 170°. Atomic Force Microscopy (AFM) using a Digital Instruments Nanoscope IIIa atomic force microscope in tapping mode and X-Ray Reflectivity (XRR) measurements were used to study the interfaces and surface morphology of the layers. The crystal quality and strain of the thin films were determined by ion channeling (RBS/C), X-Ray Diffraction (XRD) scans, Reciprocal Space Mapping (RSM) and Raman spectroscopy. X-ray measurements were accomplished with a high-resolution Bruker D8 diffractometer, employing a scintilation counter with slits of 0.05-0.1 mm. The scans were carried out with angular resolutions of 0.01-0.02°, allowing to ascertain the film thicknesses with a precision of +/- 1 nm in the XRR measurements. In the RSMs - measured around the 224 reflection - the lattice constants are determined with an accuracy of +/- 0.005 Å.

3. Results and discussion

Recently, Camacho *et al.* [15] demonstrated an electrically pumped Ge laser using a slightly tensely strained (0.25%) active layer which was heavily P doped ($7\text{x}10^{19}$ cm^{-3}). The lasing threshold is, however, very high, about $280\,\text{kA/cm}^2$ which excludes practical applications. Here, we propose a double heterostructure suitable for lasing consisting of SiGeSn cladding layers and highly biaxial tensely strained Ge as active medium, as sketched in Fig. 1a. Our approach rests upon the achievement of a strain induced quasi-direct bandgap in Ge without the need of doping. Conform to simulation this is possible if Ge layers are grown on a larger lattice, for example a fully relaxed $Ge_{0.9}Sn_{0.1}$. The SiGeSn/sGe double heterostructure is then grown pseudomorphically on top of a fully relaxed $Ge_{0.9}Sn_{0.1}$ buffer. The high tensile biaxial strain induced in the Ge layer shifts the lowest conduction bands in Ge to $E_\Gamma = 547\,\text{meV}$ and $E_L = 582\,\text{meV}$ [1], resulting in a direct bandgap (zero energy at valence band maximum). Based on electronic band structure calculations using the supercell empirical pseudopotential method [16] along with linear interpolation of deformation potentials and band-offsets of elemental Si, Ge and Sn, we determined the Si and Sn concentrations which offer quantum-well structures with band-offsets of about 50 meV and type I hetero-junctions. Here, the Si content was varied between 0 and 20 at.% whereas Sn concentrations of up to 10 at.% were used. In Fig. 1b the results of the bandgap calculations are presented: the blue surface represents the bandgap of SiGeSn cladding layers at the Γ-point of the Brillouin zone and the red plane marks the bandgap of 547 meV for strained Ge. To obtain appropriate band-offsets for population inversion, SiGeSn layers with Si concentrations above 8 at.% are required and at the same time the Sn content has to be lower than the Si content.

Previous growth studies of SiGe and GeSn have shown that the precursor combination used here is suitable for growth temperatures as low as 375°C [13]. Really low growth temperatures are essential for Sn based alloys in order to avoid surface precipitations. Here we

present the epitaxial growth of SiGeSn ternaries on Si(100) and Ge buffered Si substrates at temperatures between 350°C and 475°C. In Fig. 2, the growth rate of SiGeSn and GeSn layers on both Si(100) and Ge buffered Si(100) is shown as a function of the inverse absolute temperature, for T = 350-450°C. In this regime, the growth rate strongly depends on the temperature indicating a kinetically limited growth regime [13]. All layers have been grown at constant partial pressures (SiGeSn: p_{Si2H6} = 60 Pa, p_{Ge2H6} = 120 Pa, p_{SnCl4} = 0.6 Pa and GeSn: p_{Ge2H6} = 120 Pa, p_{SnCl4} = 0.6 Pa). The activation energy for GeSn and SiGeSn alloys is determined by exponential fits of the experimental data (dotted lines in Fig.2). The extracted values amount to about 600-700 meV for both materials. Whereas the activation energy for GeSn and SiGeSn do not vary significantly, the growth rate is doubled for GeSn compared to SiGeSn. In addition, slightly higher growth rates for SiGeSn were observed on Ge than on Si(100) substrates.

RBS channeling measurements were performed to analyse the crystal quality of the ternary alloys. Random and aligned spectra of SiGeSn layers grown (a) at 425°C on Si(100) and (b) at 350°C on a Ge buffered Si(100) substrate are shown in Figs. 3a and b, respectively. Low minimum yield values, χ_{min}, (ratio of aligned to random spectra) of about 15% for all three elements (see the insets) indicate single crystalline quality and high substitutionality of Si and Sn atoms in the Ge lattice (both layers). The Si and Sn concentrations, extracted using RUMP simulation software amount to 12 at.% and 4 at.%, respectively for the layer grown at 425°C (Fig. 3a). The lattice constant close to that of Ge, as measured by RSM demonstrates the lattice compensation effect of Si and Sn atoms. Due to the large lattice mismatch between this SiGeSn layer and the Si(001) substrate de-channeling is observed at the SiGeSn/Si interface (~1.08 MeV) typically observed for strain relaxed layers where misfit dislocations are formed at the interface. The Si and Sn concentrations of 5 at.% and 11 at.%, respectively, were obtained for the SiGeSn layer grown at 350°C on Ge (Fig. 3b).

6

For the band engineering of SiGeSn/sGe heterostructures for optoelectronic devices, it is essential to adjust the Sn and Si contents precisely in order to achieve the proper band-alignment. Adding more Sn for constant Si content results in higher lattice constants and lower bandgaps. For $Si_xGe_{1-x-y}Sn_y$ cladding layers, Si concentrations x > 8 at.% and x > y have to be achieved. Similarly to previous GeSn growth studies [13], we have observed strong temperature dependences for the Si and Sn concentrations in SiGeSn layers, as shown in Fig. 4. The Sn content increases as the growth temperatures decreases (full blue triangles). 1at.% Sn is measured for layers grown at 475°C; meanwhile, a nine times higher content is obtained at 375°C. We attribute this effect mainly to the lower cracking efficiency of Si_2H_6 as indicated in Fig. 4 where the Si content decreases as the temperature decreases (open blue triangles). Within the mentioned temperature window the Si concentration ranges between 4 at.% at 375°C and 19 at.% at 475°C for layers grown on Si(100). No significant variations of Si and Sn concentrations are observed if Ge virtual substrates are used (full and open red triangles). Interestingly, epitaxial growth is possible on Ge VS even at lower temperatures resulting in a Sn content of 12 at.% at 350°C. By contrast, growth was impossible on Si(100). For all layers presented in this section low χ_{min} values have been extracted indicating single crystalline growth and high substitutionality. No Sn surface precipitations have been observed. Growth temperature was indeed low enough to avoid Sn segregation [13]. All layers grown at temperatures ≥ 400°C (shaded area in Fig. 4a) are convenient to be employed as cladding layers in the quantum-well laser structure shown in Fig. 1. We will then have band-offsets of at least 50 meV and a type I band-alignment.

The Sn content in SiGeSn ternary and GeSn binary alloys grown on Si(100) at constant partial pressures is shown in Fig. 4b as a function of the growth temperature. This comparison shows that adding Si_2H_6 results in a significant Sn concentration increase in the grown layers. The Sn concentration is indeed whatever the growth temperature about two

7

times higher in ternary SiGeSn alloys than in GeSn alloys. At the same time, as discussed above (Fig. 2), the growth rate for GeSn is twice as high as the growth rate for SiGeSn.

A similar effect was observed by increasing the Si_2H_6 partial pressure at constant growth temperature. Fig. 5a shows the Si and Sn contents in SiGeSn layers grown at 450°C with different Si_2H_6 partial pressures (in the 0 - 90 Pa range), the Ge_2H_6 and $SnCl_4$ partial pressures being constant at 120 and 0.6 Pa, respectively. The Fig. 5a insets show the Sn signals of the RBS random spectra for alloys grown with $p_{Si2H6} = 0$ Pa (dashed lines) and 60 Pa (straight lines). The Si concentration increases by a factor of 5 if the Si_2H_6 partial pressure is increased by a factor 3 whereas the Sn content increases only by a factor of about 2. However, the χ_{min} value degrades significantly (about 50%) for $p_{Si2H6} = 90$ Pa, indicating a severe layer quality degradation. Moreover, the higher the Si_2H_6 mass-flow in the reactor, the lower the growth rate will be, see Fig. 5b. Two times higher growth rates thus lead in Fig. 5 to a two times lower Sn concentrations. The same conclusion than in Fig. 4 is thus reached.

Low growth temperatures and high Si_2H_6 mass-flows thus yield high Sn contents (for a given $SnCl_4$ partial pressure); however, the growth rate is then low. Achieving high Si contents obviously requires high Si_2H_6 mass-flows and is easier at high temperatures. A complex trade-off in terms of process conditions, especially concerning the growth temperature, will thus have to be identified for each combination of Si and Sn contents aimed for.

A critical issue concerning device fabrication is the surface roughness of the grown layers. Sn precipitation is the main effect affecting the surface roughness in Sn-based materials. The evaluation of surfaces and interfaces was carried out by XRR and AFM, as shown in Fig. 6. For SiGeSn layers grown directly on Si(100), clearly defined XRR thickness fringes are present even at high incidence angles (see Fig. 6a), indicating that layers are smooth. This is complemented by AFM root mean square (rms) roughness values between

1.4 nm and 1.6 nm. Excellent surface roughness values were otherwise associated with SiGeSn layers grown on high quality 2.5 µm thick Ge virtual substrates (which are themselves smooth: rms values below 1 nm) [17]. For all SiGeSn layers with thicknesses between 45 and 65 nm grown on those Ge virtual substrates at temperatures between 350°C and 450°C rms values were indeed in-between 0.5 nm and 0.75 nm, see Fig. 6b. The inset of Fig 6b shows a typical AFM image of the surface of a layer grown at 450°C with Si and Sn contents of 18 at.% and 4 at.%, respectively. The profile resulting from an omega-2theta scan around the (004) XRD order for a $Si_{0.08}Ge_{0.86}Sn_{0.06}$ layer grown at 400°C on a Ge VS is presented in Fig. 7a. The well-defined thickness fringes around the well-defined, intense SiGeSn peak, which it itself at a lower angle than the Ge virtual substrate peak, prove that growth was pseudomorphic and of high crystalline quality. The layer is under biaxial compressive strain due to high incorporated Sn content, confirmed also by the corresponding Raman spectrum (inset) where the sharp Ge-Ge and Si-Ge peaks are red shifted. Final proof for the high crystalline quality and atoms substitutionality is the χ_{min} value of 7% in RBS, which is close to those obtained for state-of-the-art SiGe layers. A Reciprocal Space Map around the (224) XRD order, Fig. 7b, allows the precise determination of in-plane and out-of-plane lattice constants of this ternary alloy. Pseudomorphic growth is once again proven by the identical in-plane lattice constants for the Ge virtual substrate and the SiGeSn layer (5.665 Å). We otherwise see that, while containing large amounts of Si and Sn (8 at. % and 6 at. %, respectively), this SiGeSn layer is not that lattice-mismatched with the Ge virtual substrate underneath. The perpendicular lattice parameter of the SiGeSn layer is indeed 5.709 Å, while the corresponding value for the Ge virtual substrate is 5.654 Å. Such a layer matches the barrier layer requirements for a laser heterostructure.

4. Conclusions

In conclusion, we presented electronic band-structure calculations in order to determine the appropriate Sn and Si concentrations for SiGeSn cladding layers in double heterostructure laser designs with a tensely strained Ge core. For Si concentrations ≥ 8at.% that are higher than the Sn contents, type I heterostructures with band-offsets of 50 meV can be achieved. Using a combination of Si_2H_6, Ge_2H_6 and $SnCl_4$, SiGeSn layers possessing the appropriate stoichiometry have been grown for temperatures ≥ 400°C. XRD scans along with AFM measurements demonstrated the high single crystalline quality and smooth surface morphology of those layers.

References

[1]   S. Wirths, A.T. Tiedemann, Z. Ikonic, P. Harrison, B. Holländer, T. Stoica, G. Mussler, M. Myronov, D. Buca, S. Mantl, Applied Physics Letters 102 (2013) 192103.

[2]   R. Kotlyar, U.E. Avci, S. Cea, R. Rios, T.D. Linton, K.J. Kuhn, I. A. Young, Applied Physics Letters 102 (2013) 113106.

[3]   K. Kao, A. Verhulst, W. Vandenberghe, B. Sorée, G. Groeseneken, K. De Meyer, IEEE Transactions on Electron Devices 59 (2012) 292.

[4]   J. Liu, D. Cannon, K. Wada, Y. Ishikawa, D. Danielson, S. Jongthammanurak, J. Michel, L. Kimerling, Physical Review B 70 (2004) 155309.

[5]   P. Moontragoon, Z. Ikonić, P. Harrison, Semiconductor Science and Technology 22 (2007) 742.

[6]   R. Chen, H. Lin, Y. Huo, C. Hitzman, T.I. Kamins, J.S. Harris, Applied Physics Letters 99 (2011) 181125.

[7]   M. El Kurdi, G. Fishman, S. Sauvage, P. Boucaud, Journal of Applied Physics 107 (2010) 013710.

[8]   J. Xie, A.V.G. Chizmeshya, J. Tolle, V.R. D'Costa, J. Menendez, J. Kouvetakis, Chemistry of Materials 22 (2010) 3779.

[9]   H. Lin, R. Chen, W. Lu, Y. Huo, T.I. Kamins, J.S. Harris, Applied Physics Letters 100 (2012) 141908.

[10]   J.P. Fleurial, A. Borshchevsky, Journal of The Electrochemical Society 137 (1990) 2928.

[11]   M. Bauer, C. Ritter, P. a. Crozier, J. Ren, J. Menendez, G. Wolf, J. Kouvetakis, Applied Physics Letters 83 (2003) 2163.

[12]   R.T. Beeler, C. Xu, D.J. Smith, G. Grzybowski, J. Menéndez, J. Kouvetakis, Applied Physics Letters 101 (2012) 221111.

[13]   S. Wirths, D. Buca, G. Mussler, A. T. Tiedemann, B. Holländer, P. Bernardy, T. Stoica, D. Grutzmacher, S. Mantl, ECS Journal of Solid State Science and Technology 2 (2013) N99.

[14]   S. Wirths, D. Buca, A.T. Tiedemann, P. Bernardy, B. Holländer, T. Stoica, G. Mussler, U. Breuer, S. Mantl, Solid-State Electronics 83 (2013) 2.

[15]   R.E. Camacho-Aguilera, Y. Cai, N. Patel, J.T. Bessette, M. Romagnoli, L.C. Kimerling, J. Michel, Optics Express 20 (2012) 11316.

[16] P. Moontragoon, P. Pengpit, T. Burinprakhon, S. Maensiri, N. Vukmirovic, Z. Ikonic, P. Harrison, Journal of Non-Crystalline Solids 358 (2012) 2096.

[17] J.M. Hartmann, A. Abbadie, N. Cherkashin, H. Grampeix, L. Clavelier, Semiconductor Science and Technology 24 (2009) 055002.

Figure captions :

Figure 1 : (a) Layer structure of the proposed fully strained double heterostructure laser. The relaxed $Ge_{0.9}Sn_{0.1}$ buffer serves as a stressor layer for Ge. (b) Bandgaps of the strained Ge (red surface) and $Si_xGe_{1-x-y}Sn_y$ cladding layers (blue surface) at the Γ-point of the Brillouin zone as a function of the Si and Sn concentration.

Figure 2 : Arrhenius plot of (i) the SiGeSn epitaxial growth rate on Si(100) (blue squares) and Ge buffered Si (red circles) and (ii) of the GeSn epitaxial growth rate on Si(100) (green triangles) at constant precursor partial pressures.

Figure 3 : RBS random and aligned spectra for (a) 45 nm $Si_{0.12}Ge_{0.84}Sn_{0.04}$ grown at 425°C and (b) 85 nm $Si_{0.04}Ge_{0.85}Sn_{0.11}$ grown at 350°C on Si(100).

Figure 4 : (a) Si and Sn content as a function of the growth temperature on Si(100) and Ge buffered Si. The shaded area denotes suitable Si to Sn ratios for SiGeSn cladding layers. (b) Sn concentration as a function of the growth temperature for SiGeSn and GeSn growth on Si(100). Si_2H_6, Ge_2H_6 and $SnCl_4$ partial pressures were fixed: 60, 120 and 0.6 Pa, respectively. The SiGeSn layer thicknesses amount between 50 nm and 100 nm.

Figure 5 : (a) Si and Sn content as a function of the Si_2H_6 partial pressure at 450°C. The insets show the Sn signals of the RBS random spectra. (b) SiGeSn Growth rate for different Si_2H_6 partial pressures at 450°C. Ge_2H_6 and $SnCl_4$ partial pressures were constant: 120 and 0.6 Pa, respectively.

Figure 6 : (a) XRR curves for several SiGeSn layers grown on Si(100) at 425°C (blue), 400°C (green) and 375°C (red). The layer thicknesses extracted from those XRR curves are 54 nm, 78 nm and 45 nm, respectively. (b) Root mean square (RMS) values determined by AFM for 45 - 65 nm thick SiGeSn layers grown at different temperatures on Ge virtual substrates. The inset shows an AFM image of a 65 nm thick SiGeSn layer grown at 450°C on Ge.

Figure 7 : (a) Omega-2Theta scan around the (004) XRD order and Raman spectrum (inset) of a 55 nm thick $Si_{0.08}Ge_{0.86}Sn_{0.06}$ layer grown 400°C on a Ge virtual substrate. The Ge-Ge line is based on measurements on Ge bulk and the Si-Ge line is for SiGeSn layer as used also by [11]. (b) Reciprocal Space Map around the (224) XRD order of the same $Si_{0.08}Ge_{0.86}Sn_{0.06}$ layer grown on a Ge virtual substrate.
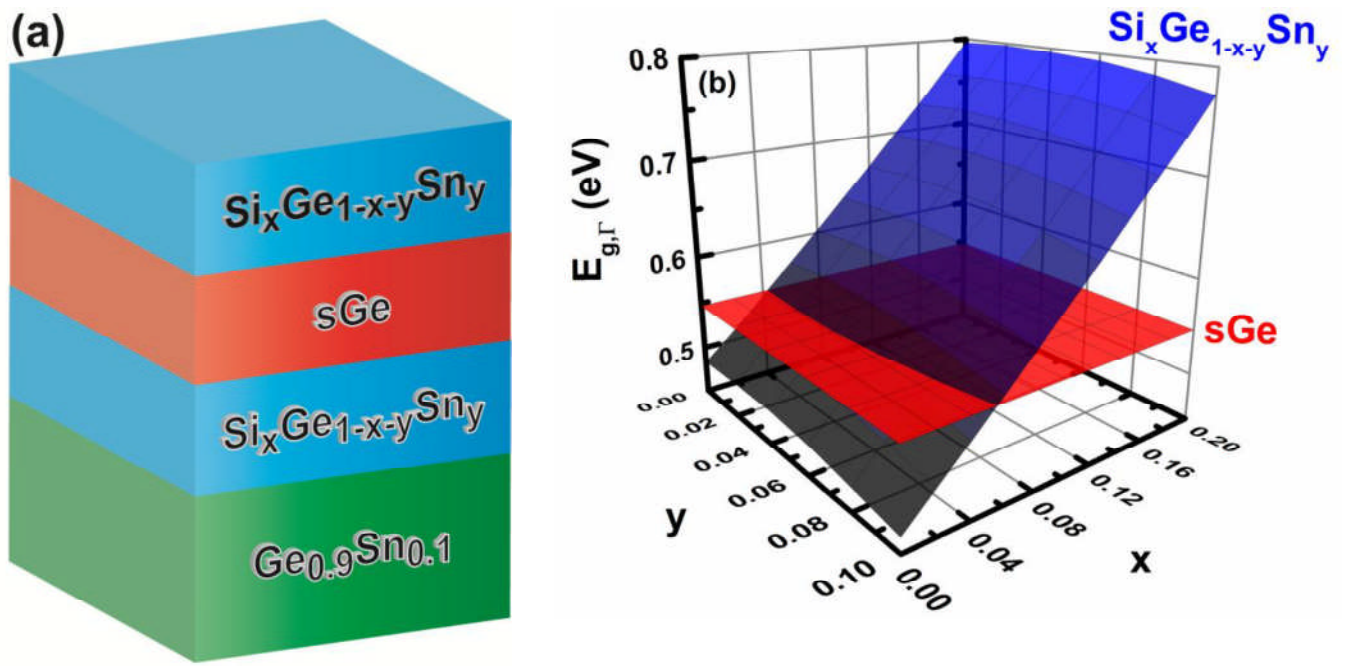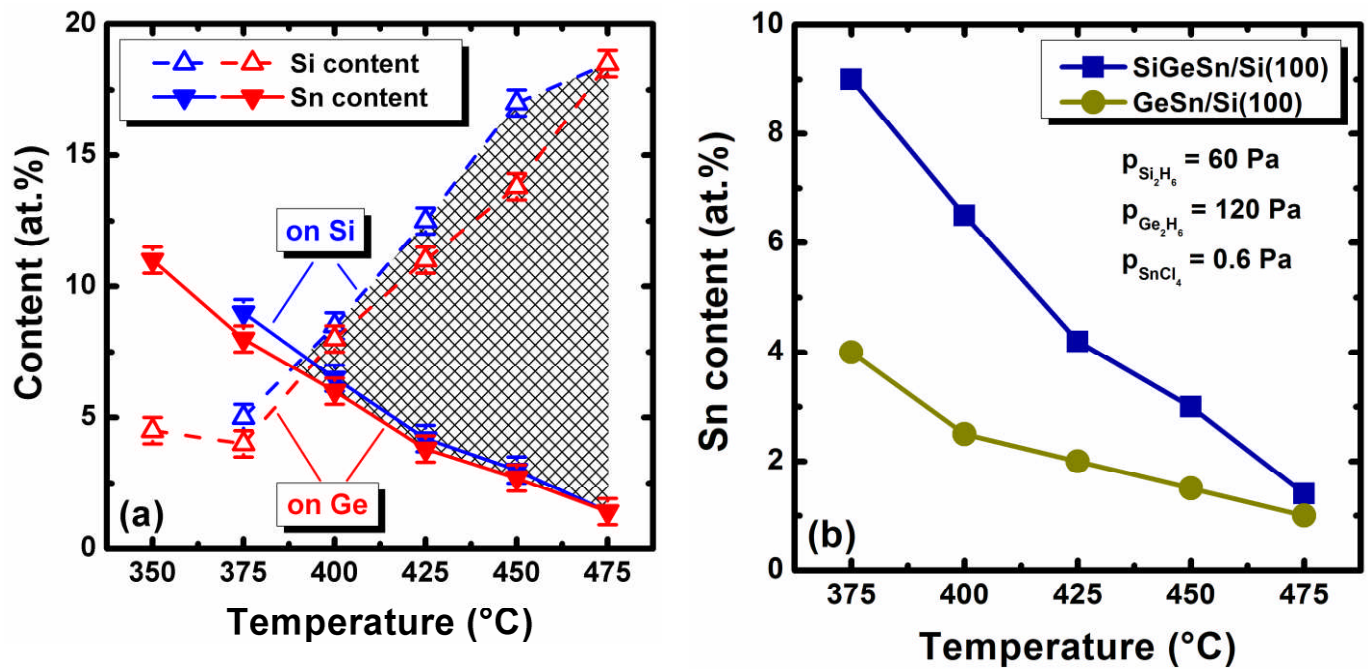
Figure 1:
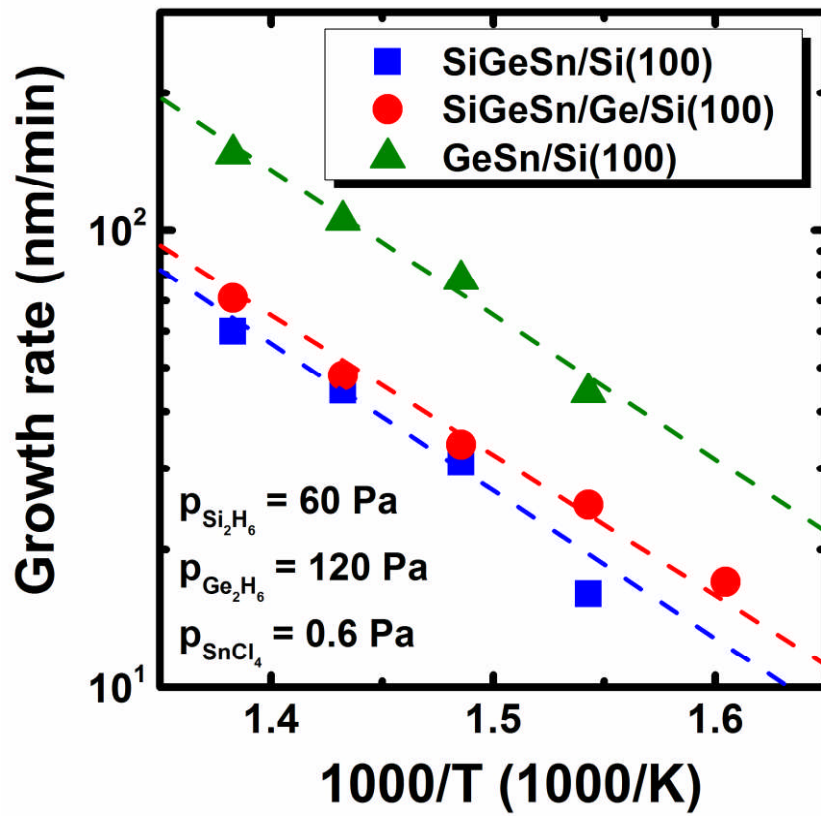
Figure 2:
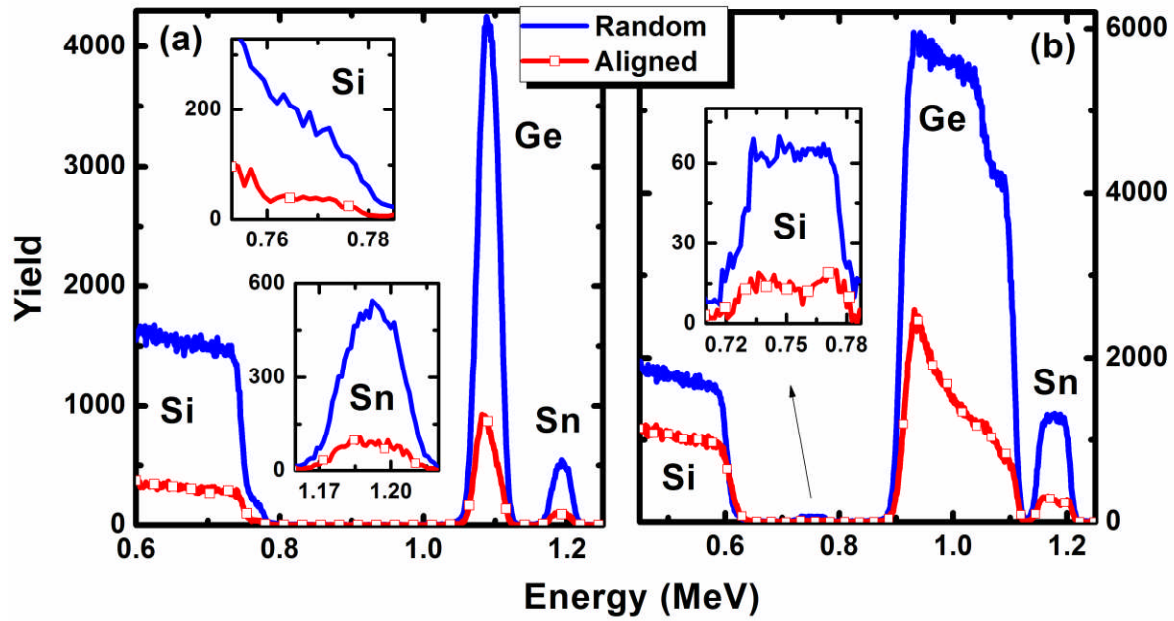
Figure 3:

Figure 4:
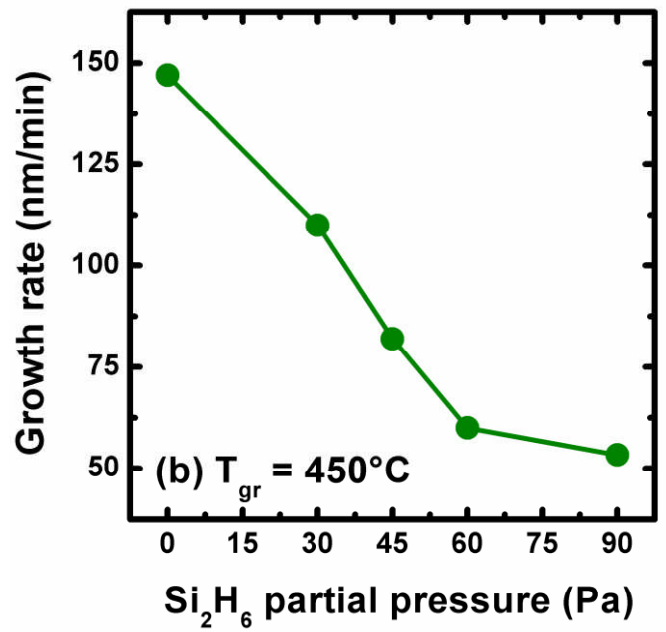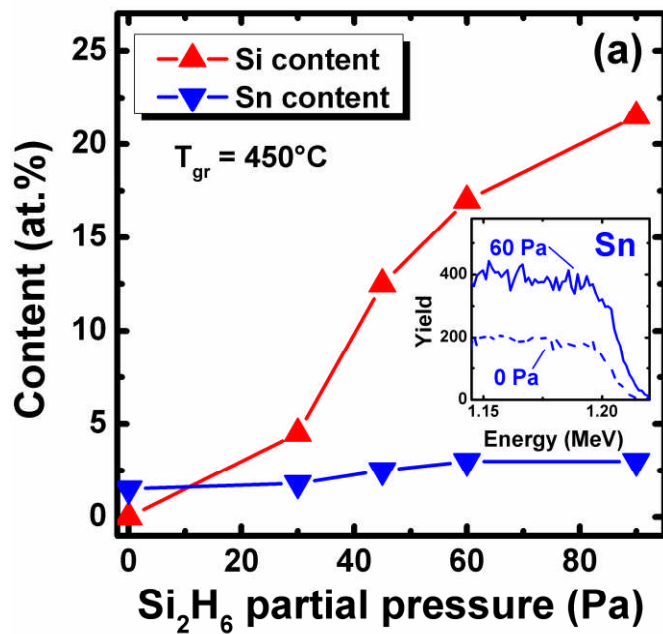
Figure 5:

Figure 6:

Figure 7: